

Electronic Supplementary Information

Photoswitchable organic field-effect transistors and memory elements comprising interfacial photochromic layer

Lyubov A. Frolova, Pavel A. Troshin*, Diana K. Susarova, Alexander A. Kulikov, Nataliya A. Sanina and Sergey M. Aldoshin

Contents

Experimental procedure	2
Fig. S1. Transfer characteristics of photoswitchable OFET obtained under illumination of devices under zero bias with violet and green light (pure photoswitching effect).	3
Fig. S2. Transfer characteristics of the photoswitchable OFETs as a function of the programming time in the forward (a) and backward (b) directions. The device drain current at $V_{GS}=1.1$ V as a function of the programming time in the forward and backward directions (c).	4
Fig. S3. Transfer characteristics of the photoswitchable OFETs obtained using blue (a), green (b) and red (c) light while applying different programming voltages	5
Fig. S4. Evolution of the reflectance spectra of the ITO/SpOx/Ag (a) and ITO/SpOx/C ₆₀ /Ag (b) diodes under illumination with light (405 nm) and/or applying electrical bias.	6
Fig. S5 The reflectance spectra of the ITO/C ₆₀ /Ag diodes under illumination with light (405 nm) and/or applying electrical bias.	7
Fig. S6. Absorption spectra of the C ₆₀ , SpOx and SpOx/C ₆₀ thin films. Red arrows highlight the broad absorption bands corresponding to the CT states formed at the interface between SpOx and C ₆₀ layers	8
Table S1. Comparison of the results obtained in this work with the previously published literature data on the memory devices based on organic photochromic materials	9

Experimental procedure

The photoswitchable OFETs and memory devices were fabricated on glass substrates. The glass slides were cleaned by sonication in a base piranha solution (a mixture of hydrogen peroxide and ammonia, both obtained from ChimMed, Russia), rinsed with deionized water and dried in an oven at 60°C for 30 min. Aluminium gate electrodes with a thickness of 200 nm were deposited by thermal evaporation in vacuum (2×10^{-6} mbar) through a shadow mask. Afterwards, AlO_x was grown by anodic oxidation of aluminum gate electrodes in 0.01 mol citric acid (Acros Organics) at constant potential of 12 V. Afterwards, the samples were rinsed with deionized water and dried in a vacuum oven at 60°C for 30 min. A toluene solution of spirooxazine (obtained from Sigma-Aldrich, concentration 10 mg ml⁻¹) was spin coated at 750 rpm onto the aluminum oxide layer inside a nitrogen glove box. Then the samples were transferred to the vacuum chamber (also integrated inside glove box) and [60]fullerene was thermally deposited with a rate of 0.3–0.4 nm s⁻¹ at 320°C under vacuum (2×10^{-6} mbar) to form a 100 nm thick semiconductor layer. The devices were finalized by evaporating 100 nm thick silver source and drain electrodes through a shadow mask. The channel length (L) and width (W) were 50 and 2000 μm, respectively.

The electrical characterization of the devices was performed using double-channel Keithley 2612A instrument. Diode lasers with a power of ~ 20 mW and sharp maxima at 405 nm (violet), 450 nm (blue), 532 nm (green) and 650 nm (red) provided illumination required for programming the memory elements.

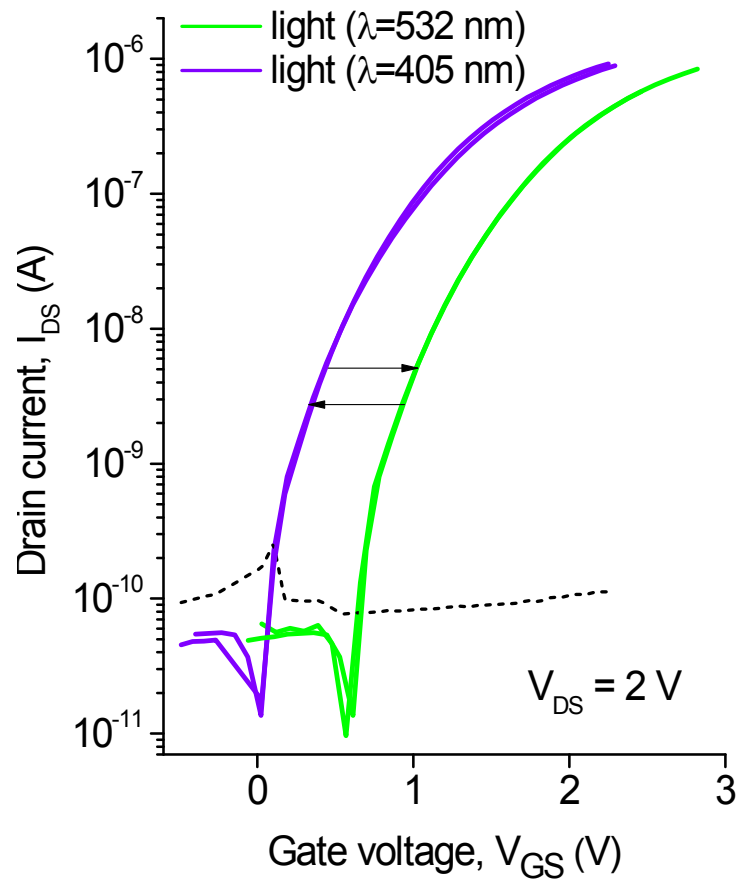


Fig. S1. Transfer characteristics of photoswitchable OFET obtained under illumination of devices under zero bias with violet and green light (pure photoswitching effect).

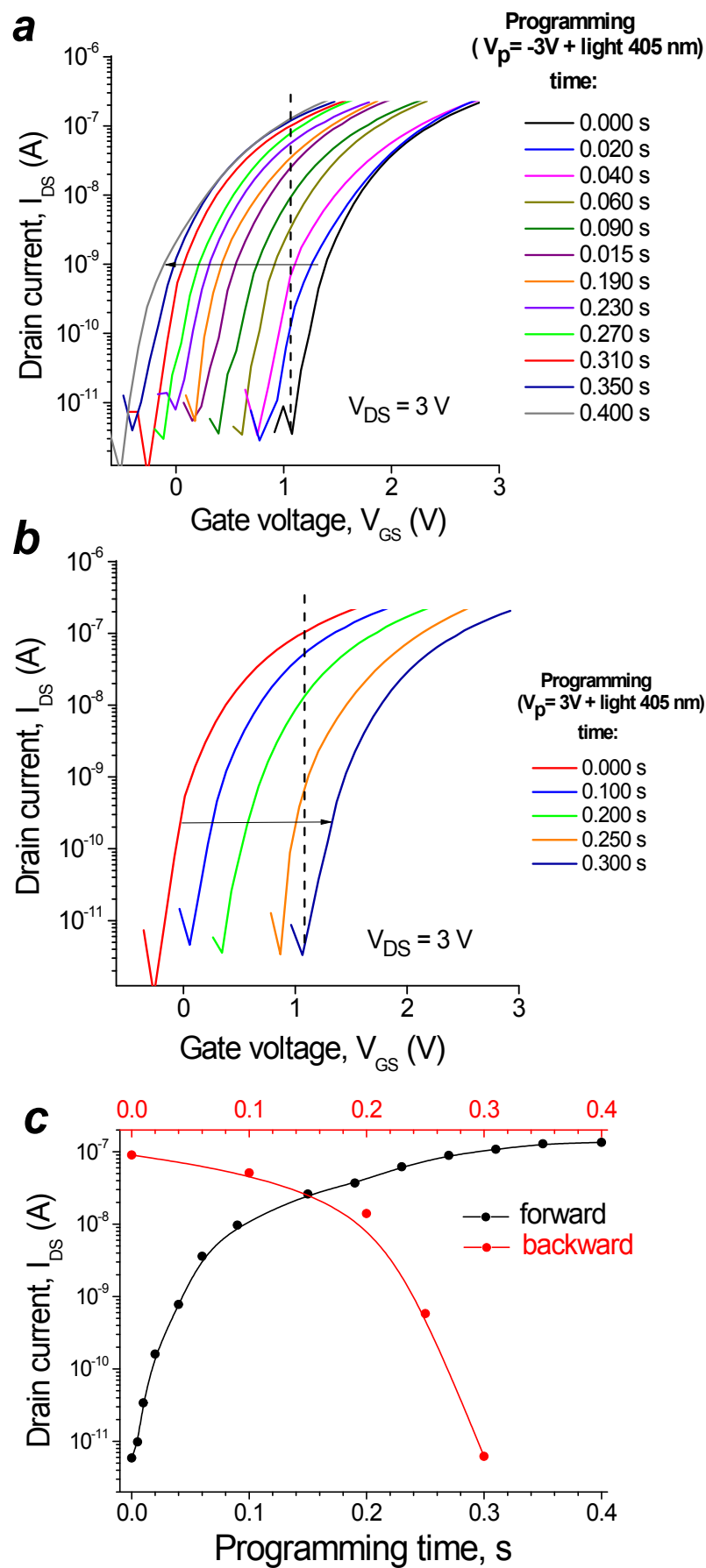


Fig. S2. Transfer characteristics of the photoswitchable OFETs as a function of the programming time in the forward (a) and backward (b) directions. The device drain current at $V_{GS}=1.1 \text{ V}$ as a function of the programming time in the forward and backward directions (c).

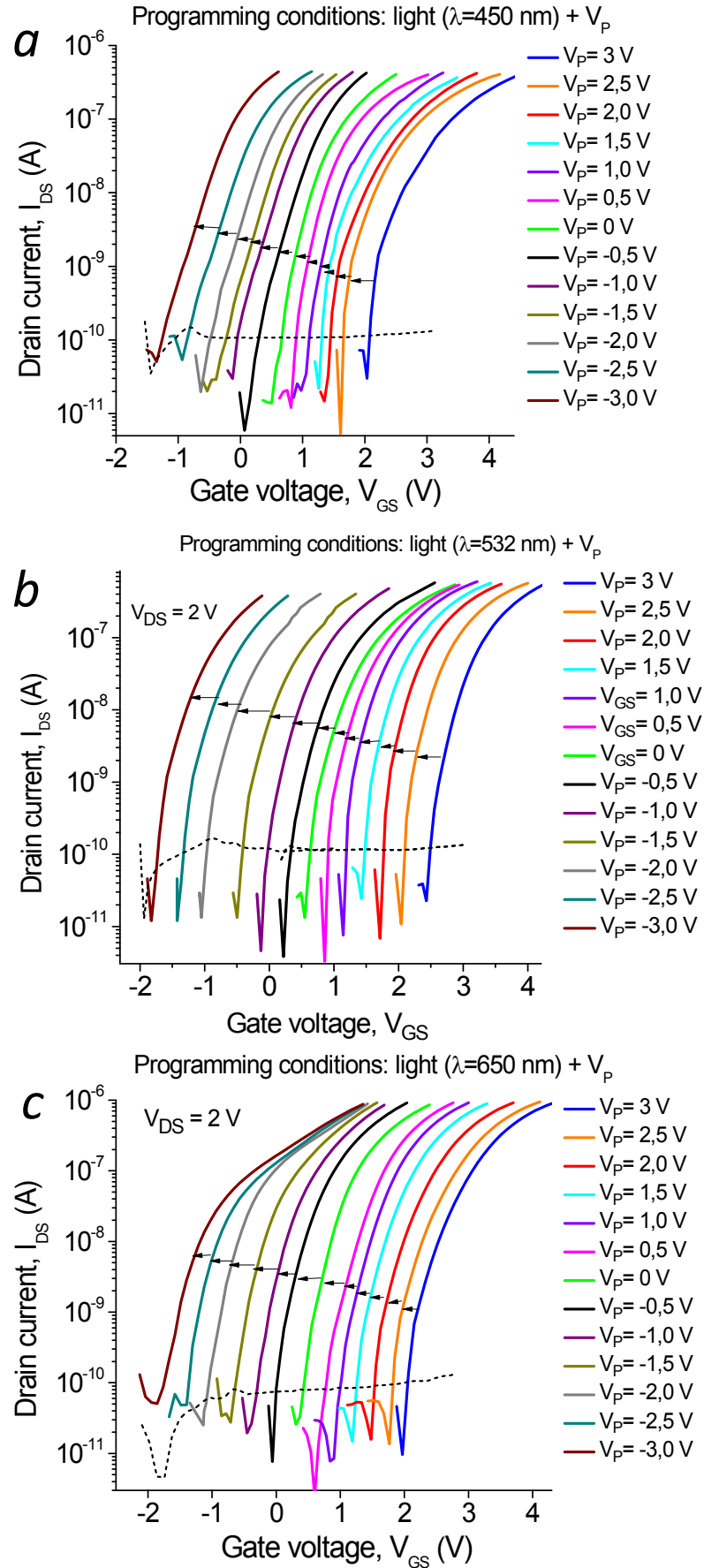


Fig. S3. Transfer characteristics of the photoswitchable OFETs obtained using blue (a), green (b) and red (c) light while applying different programming voltages

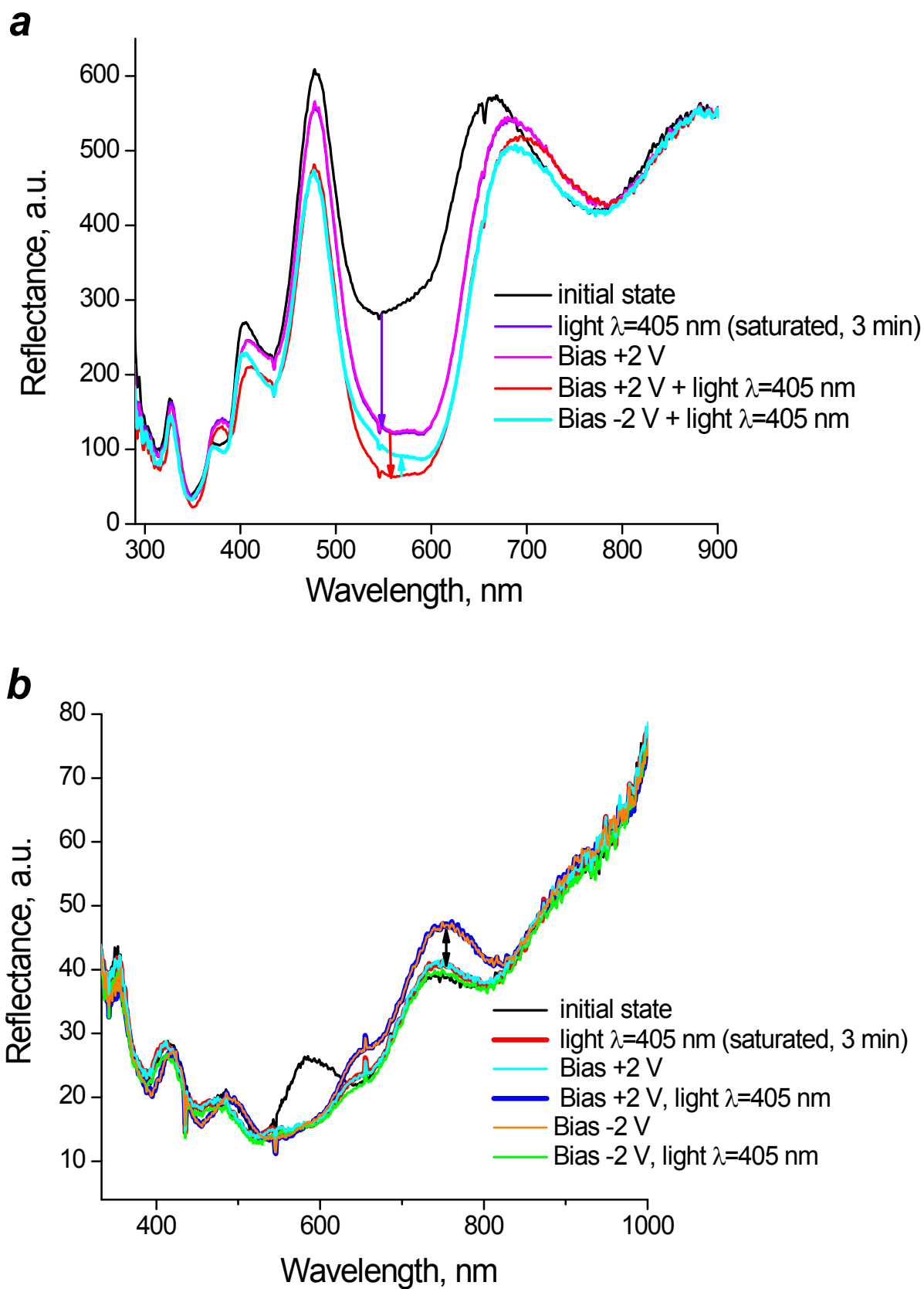


Fig. S4. Evolution of the reflectance spectra of the ITO/SpOx/Ag (a) and ITO/SpOx/C₆₀/Ag (b) diodes under illumination with light (405 nm) and/or applying electrical bias.

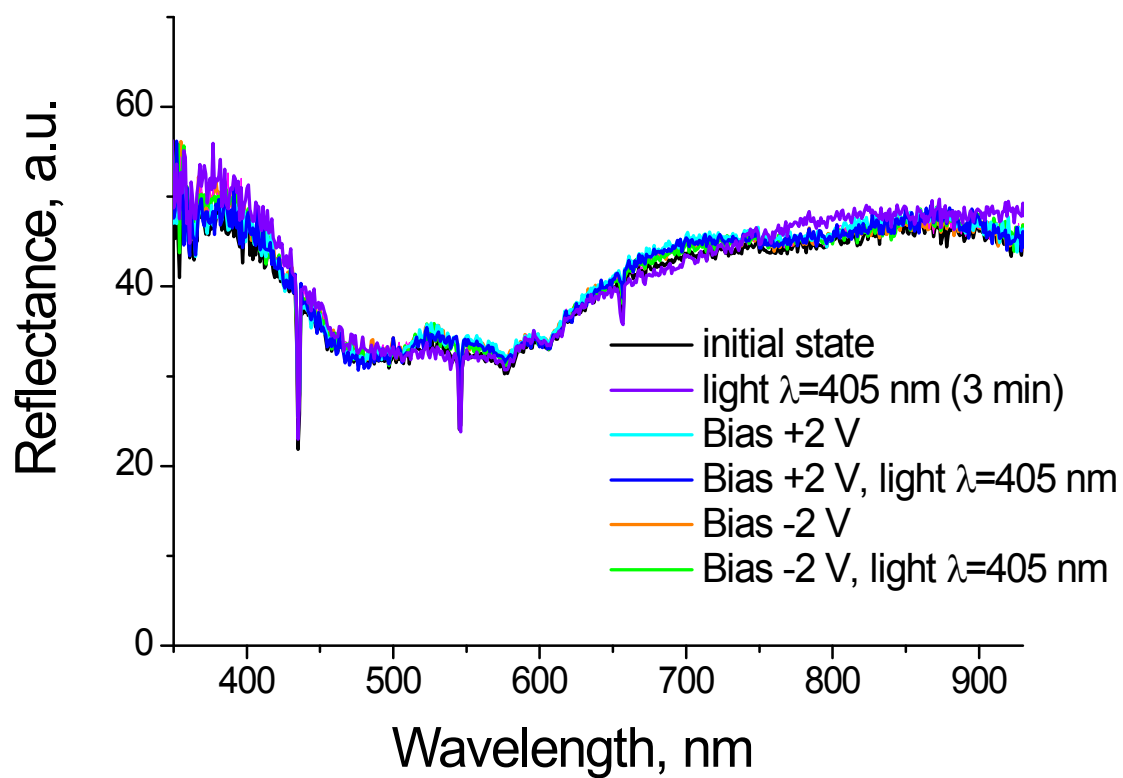


Fig. S5 The reflectance spectra of the ITO/C₆₀/Ag diodes under illumination with light (405 nm) and/or applying electrical bias.

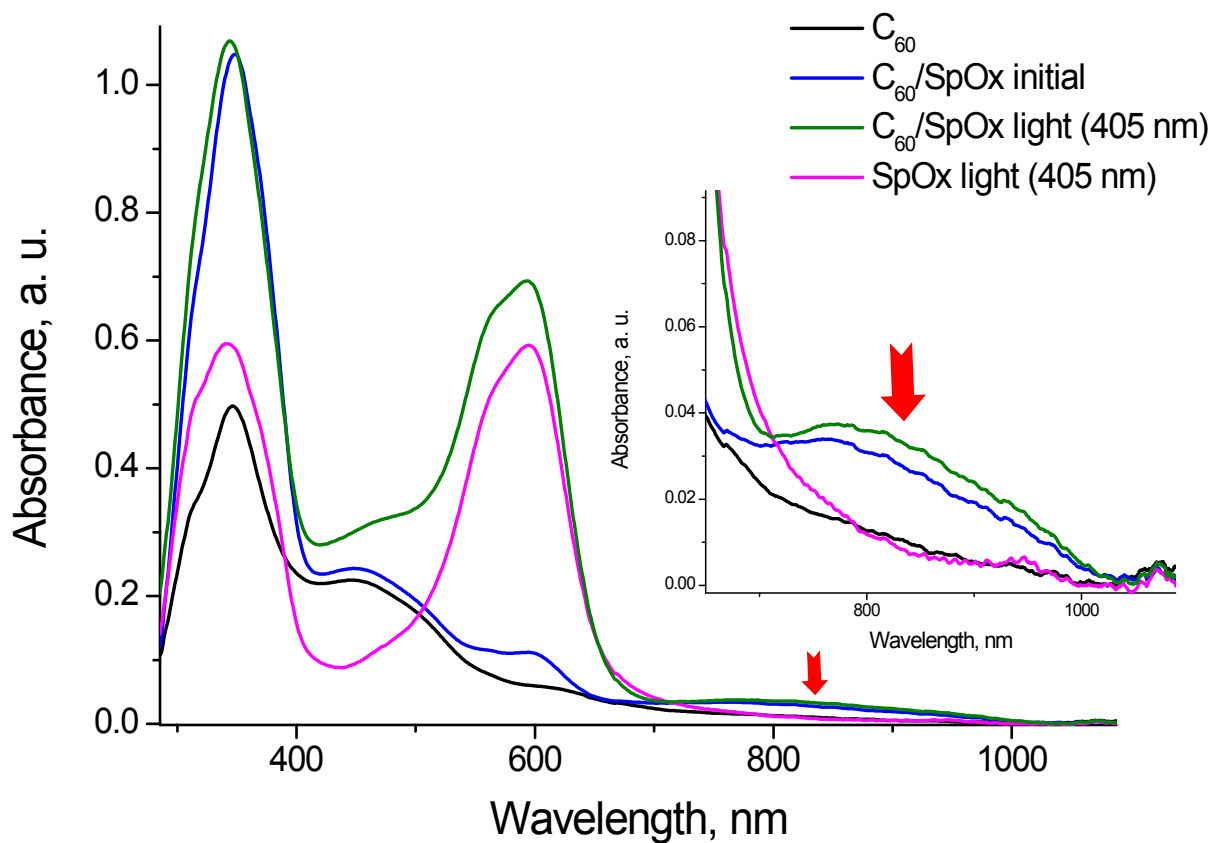
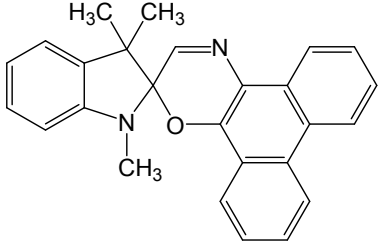
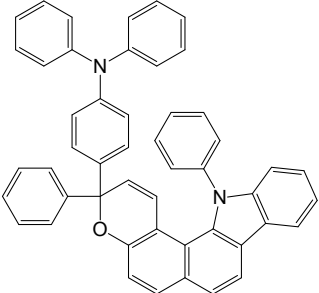
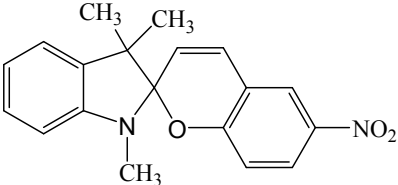
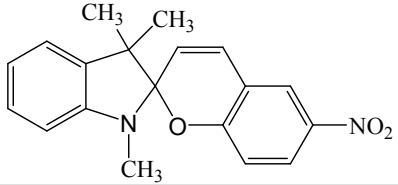
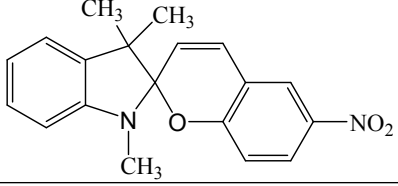
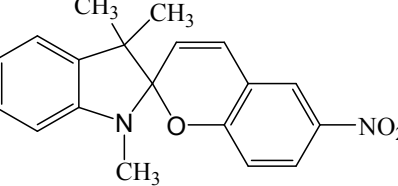
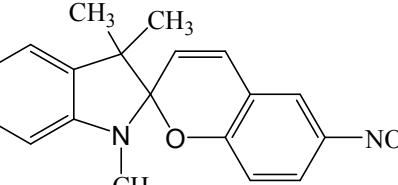
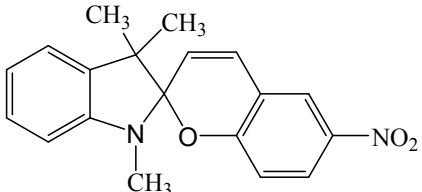
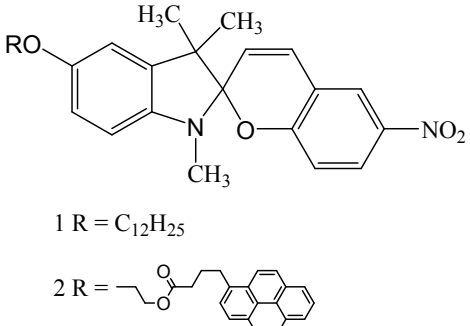
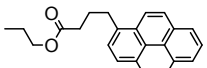
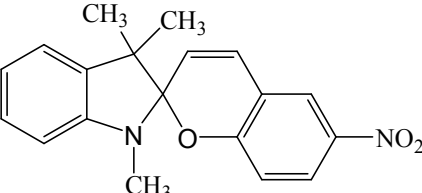
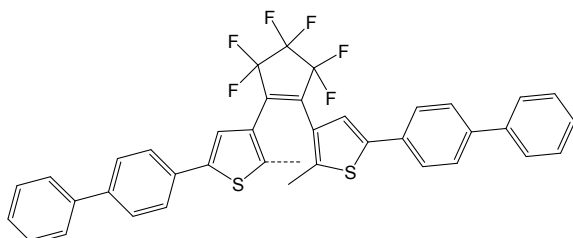
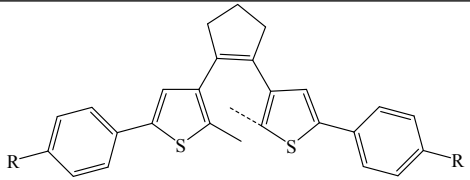
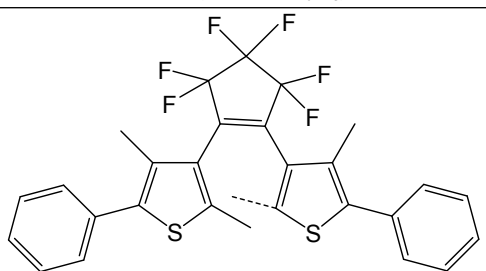
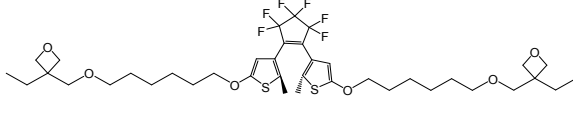
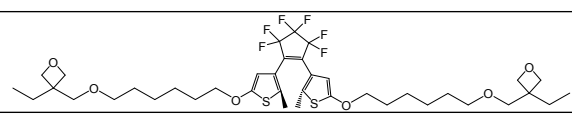
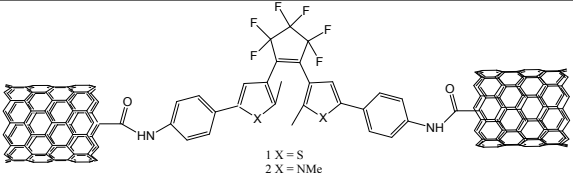
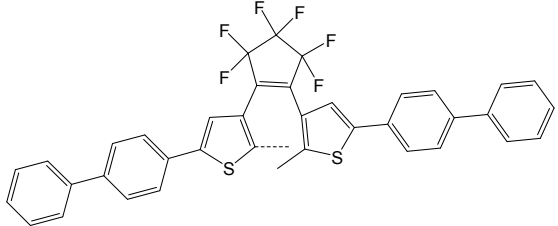
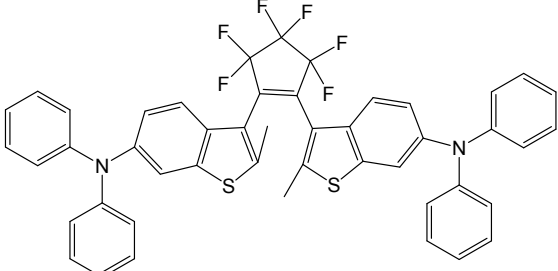
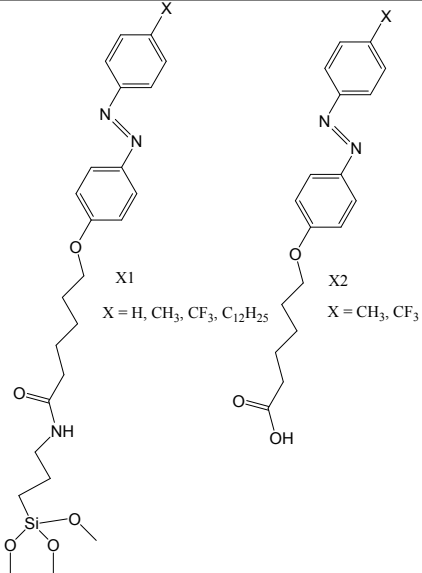
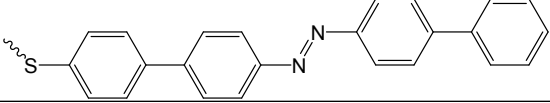
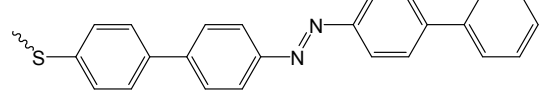


Fig. S6. Absorption spectra of the C_{60} , SpOx and SpOx/ C_{60} thin films. Red arrows highlight the broad absorption bands corresponding to the CT states formed at the interface between SpOx and C_{60} layers

Table S1. Comparison of the results obtained in this work with the previously published literature data on the memory devices based on organic photochromic materials

Entry	Photochromic material	Switching time	Switching coefficient $k_{sw}=I_{DS}(\text{state 1})/I_{DS}(\text{state 2})$	Switching conditions	Type of the device	Ref.
0		0.02-0.5 s	10-10000	Visible light + bias (3 V)	OFET	This work
1		~30 min	~1.2	UV (F)* VIS (B)	OFET	[1]
2		~30 min	~1.8	UV (F) VIS (B)	OFET	[2]
3		~30 min	~1.4	UV, bias	Dual-channel OFET	[3]
4		~200 s	~1.002	UV (F) VIS (B)	OFET	[4]
5		10 s - 1200 s	~1.03-3.0	UV (F) VIS (B)	OFET	[5]
6		~1-2 min	1.2-2.0	UV	OFET	[6]

7		<p>~10-40 s ~200-600 s</p>	<p>~1.3 ~2.0</p>	<p>UV (F) VIS (B)</p>	OFET	[7]
8	 <p>1 R = C₁₂H₂₅ 2 R = </p>	~800 s	~2.6	<p>UV (F) VIS (B)</p>	OFET	[8]
9		~20 s	~1.06	<p>UV (F) VIS (B)</p>	OFET	[9]
10		2-3 min	~100	<p>UV (F) VIS (B)</p>	OFET	[10]
11	 <p>DAE1 (R = CH₃) DAE2 (R = CO₂-<i>n</i>-C₆H₁₃)</p>	~5 s**	~1.2	<p>UV (F) VIS (B)</p>	OFET	[11]
12		~60 sec	~ 6	<p>UV (F) VIS (B)</p>	OFET	[12]
13		>2 min	~100	<p>UV Bias</p>	Diode	[13]
14		60 s	3000	<p>UV (F) VIS (B)</p>	OLED	[14]

15	 <p>1 X = S 2 X = NMe</p>	~5-10 s	~27	UV (F) VIS (B)	Lateral diode	[15]
16		2-5 min	~1.5	UV (F) VIS (B)	Diode	[16]
17		~15-250 s	~2.0	Bias	Diode	[17]
18	 <p>X1 X = H, CH₃, CF₃, C₁₂H₂₅</p> <p>X2 X = CH₃, CF₃</p>	5-40 min	~11-21	UV	OFET	[18]
		1 - 30 s	~3000-4500	electrical bias (20-100 V)		
19		~5-10 min	~6-13	UV (F) VIS (B)	OFET	[19]
20		~15 min	~3	UV (F) VIS (B)	OFETs	[20]

* Here and below “F” corresponds to forward switching and “B” to the backward transition.

** The characteristic time t_R of 3-4 μ s reported in this work corresponds most likely to the photocurrent jump signal which does not lead to any noticeable device programming effect.

References

1. Y. Ishiguro, M. Frigoli, R. Hayakawa, T. Chikyow and Y. Wakayama, *Org. Electron.*, 2014, **15**, 1891–1895.
2. Y. Ishiguro, R. Hayakawa, T. Chikyow and Y. Wakayama, *J. Mater. Chem.C*, 2013, **1**, 3012.

3. Y. Ishiguro, R. Hayakawa, T. Yasuda, T. Chikyow and Y. Wakayama, *ACS Appl. Mater. Interfaces*, 2013, **5**, 9726–9731.
4. Y. Li, H. Zhang, C. Qi and X. Guo, *J. Mater. Chem.*, 2012, **22**, 4261.
5. H. Zhang, X. Guo, J. Hui, S. Hu, W. Xu and D. Zhu, *Nano Lett.*, 2011, **11**, 4939–4946.
6. P. Lutsyk, K. Janus, J. Sworakowski, G. Generali, R. Capelli and M. Muccini, *J. Phys. Chem. C*, 2011, **115**, 3106–3114.
7. Q. Shen, L. Wang, S. Liu, Y. Cao, L. Gan, X. Guo, M. L. Steigerwald, Z. Shuai, Z. Liu and C. Nuckolls, *Adv. Mater.*, 2010, **22**, 3282–3287.
8. X. Guo, L. Huang, S. O'Brien, P. Kim and C. Nuckolls, *J. Am. Chem. Soc.*, 2005, **127**, 15045–15047.
9. Q. Shen, Y. Cao, S. Liu, M. L. Steigerwald and X. Guo, *J. P. Chem. C*, 2009, **113**, 10807–10812.
10. R. Hayakawa, K. Higashiguchi, K. Matsuda, T. Chikyow and Y. Wakayama, *ACS Appl. Mater. Interfaces*, 2013, **5**, 3625–3630.
11. E. Orgiu, N. Crivillers, M. Herder, L. Grubert, M. Pätzelt, J. Frisch, E. Pavlica, D. T. Duong, G. Bratina, A. Salleo, N. Koch, S. Hecht and P. Samorì, *Nat. Chem.*, 2012, **4**, 675–679.
12. M. Yoshida, K. Suemori, S. Uemura, S. Hoshino, N. Takada, T. Kodzasa and T. Kamata, *Jap. J. Appl. Phys.*, 2010, **49**, 04DK09.
13. R. C. Shallcross, P. O. Körner, E. Maibach, A. Köhnen and K. Meerholz, *Adv. Mater.*, 2013, **25**, 4807–4813.
14. P. Zacharias, M. C. Gather, A. Köhnen, N. Rehmman and K. Meerholz, *Angew. Chem. Int. Ed.* 2009, **48**, 4038–4041.
15. A. C. Whalley, M. L. Steigerwald, X. Guo and C. Nuckolls, *J. Am. Chem. Soc.*, 2007, **129**, 12590–12591.
16. R. Hayakawa, K. Higashiguchi, K. Matsuda, T. Chikyow and Y. Wakayama, *ACS Appl. Mater. Interfaces*, 2013, **5**, 11371–11376.
17. T. Tsujioka, N. Iefuji, A. Jiapaer, M. Irie and S. Nakamura, *Appl. Phys. Lett.*, 2006, **89**, 222102.
18. C.-W. Tseng, D.-C. Huang and Y.-T. Tao, *ACS Appl. Mater. Interfaces*, 2012, **4**, 5483–5491.
19. C. Raimondo, N. Crivillers, F. Reinders, F. Sander, M. Mayor and P. Samorì, *Proc. Nat. Acad. Sci.*, 2012, **109**, 12375–12380.
20. N. Crivillers, E. Orgiu, F. Reinders, M. Mayor and P. Samorì, *Adv. Mater.* 2011, **23**, 1447–1452.